Roles of Tyr[13] and Phe[219] in the Unique Substrate Specificity of Pepsin B[†]

Takashi Kageyama

Center for Human Evolution Modeling Research, Primate Research Institute, Kyoto University, Inuyama 484-8506, Japan

Received July 19, 2006; Revised Manuscript Received September 14, 2006

ABSTRACT: Pepsin B is known to be distributed throughout mammalia, including carnivores. In this study, the proteolytic specificity of canine pepsin B was clarified with 2 protein substrates and 37 synthetic octapeptides and compared with that of human pepsin A. Pepsin B efficiently hydrolyzed gelatin but very poorly hydrolized hemoglobin. It was active against only a group of octapeptides with Gly at P2, such as KPAGF↓LRL and KPEGF↓LRL (arrows indicate cleavage sites). In contrast, pepsin A hydrolyzed hemoglobin but not gelatin and showed high activity against various types of octapeptides, such as KPAEF↓FRL and KPAEF↓LRL. The specificity of pepsin B is unique among pepsins, and thus, the enzyme provides a suitable model for analyzing the structure and function of pepsins and related aspartic proteinases. Because Tyr[13] and Phe[219] in/around the S2 subsites (Glu/Ala[13] and Ser[219] are common in most pepsins) appeared to be involved in the specificity of pepsin B, site-directed mutagenesis was undertaken to replace large aromatic residues with small residues and vice versa. The Tyr[13]Ala/Phe[219]Ser double mutant of pepsin B was found to demonstrate broad activity against hemoglobin and various octapeptides, whereas the reverse mutant of pepsin A had significantly decreased activity. According to molecular modeling of pepsin B, Tyr[13] OH narrows the substrate-binding space and a peptide with Gly at P2 might be preferentially accommodated because of its high flexibility. The hydroxyl can also make a hydrogen bond with nitrogen of a P3 residue and fix the substrate main chain to the active site, thus restricting the flexibility of the main chain and strengthening preferential accommodation of Gly at P2. The phenyl moiety of Phe[219] is bulky and narrows the S2 substrate space, which also leads to a preference for Gly at P2, while lowering the catalytic activity against other peptide types without making a hydrogen-bonding network in the active site.

Pepsins are members of a group of aspartic proteinases, which play integral roles in the digestion processes of vertebrates. To date, five major types have been identified: pepsin A, pepsin B, gastricsin (pepsin C), chymosin, and pepsin F, which are known to have diverged from a common ancestor during evolution (*1*−*7*). The diversity suggests that each type of pepsin possesses unique actions in efficient digestion of food proteins, each with a type-specific catalytic apparatus. Pepsins have been studied extensively in the field of protein chemistry and enzymology (*8*, *9*), and pepsin A has been established as a typical model for analyzing the structure and function of proteolytic enzymes (*10*−*12*). Chymosin, which is expressed predominantly in the fetal and neonatal stages, has also been studied in detail because it is essential for milk digestion and is a prerequisite for making cheese (*2*, *13*).

In contrast to pepsin A and chymosin, the proteolytic specificities of other types of pepsins have been analyzed less extensively (*3*, *7*, *14*). Pepsin B was reported as a parapepsin in the porcine stomach in 1959 by Ryle and Porter (*15*). But, the structure and proteolytic specificity remained unknown until recently because the enzyme does not hydrolyze standard substrates for pepsin A or chymosin (*16*−*18*). To date, pepsinogen B/pepsinogen-B-like zymogen have been detected in canine (*6*, *19*), feline (*20*), and porcine (*16*−*18*) stomachs, and expression at high levels in the gastric tissues of carnivorous and omnivorous animals would be in line with adaptation for the digestion of meat that is rich in collagen. Zymogen might be less important in herbivorous mammals, including primates, and indeed, the respective gene has been found to be inactivated in the human genome (AADC01006127). In 2002, we first molecularly cloned a cDNA for pepsinogen B from the canine stomach, along with the purification of the zymogen. Pepsin B belongs to a group independent from other pepsins and is active against only a limited number of peptides, indicating a very different substrate specificity from those of other pepsins (*6*). Thus, an investigation of essential active-site residues of pepsin B should aid in elucidating the structural and functional diversity of pepsins and provide a better understanding of the forces involved in determining the specificities of proteolytic enzymes.

Pepsin specificity has been investigated using various substrates, including proteins and peptides (*9*−*11*), and extensive studies with porcine pepsin A have clarified its cleavage specificity. Earlier studies with synthetic peptides by Fruton and his colleagues demonstrated the hydrolysis of peptide bonds that connect bulky hydrophobic/aromatic

[†] This work was supported in part by Grant-in-Aid for Scientific Research (14340263) and MEXT Grant-in-Aid for the 21st Century COE Program (A2 to Kyoto University) from the Ministry of Education, Culture, Sports, Science and Technology of Japan and the JSPS-HOPE Core-to-Core Program.

* Corresponding author. Phone: +81-568-63-0578. Fax: +81-568-63-0085. E-mail: kageyama@pri.kyoto-u.ac.jp.

10.1021/bi061467a CCC: $33.50
Published on Web 11/09/2006

residues, such as Phe-Trp, Phe-Tyr, and Phe-Phe (*9*), and the accommodation of seven-residue peptides in its active site (*21*). A detailed survey of pepsin cleavage sites in 177 proteins confirmed the occurrence of hydrophobic combinations at cleavage sites (*22*). X-ray structural studies have suggested that pepsin-family members feature a large active site cleft in the center of the enzyme that contains two catalytic-site aspartates, Asp^{32} and Asp^{215} (in pepsin A numbering), and several hydrophobic residues in the neighborhood of the catalytic residues (*23*−*26*). The cleft is sufficiently long to accommodate a seven-residue substrate, constituting S4 through S3′. With a set of synthetic chromogenic peptides, Dunn et al. (*27*−*29*) elucidated the details of favorable and unfavorable amino acids at P4 through P3′ positions of substrates for pepsin A and chymosin, recommending Lys-Pro-Ala/Ile-Glu-Phe-Phe-Arg-Leu as an optimal substrate.

In parallel with protein and peptide hydrolytic analyses, site-directed mutagenesis has also been useful to explore pepsin specificity. Because subsite-forming residues are thought to have essential roles in catalysis, they, especially the S1 subsites of porcine pepsin A and bovine chymosin, have attracted attention (*30*−*35*). The S1′ subsite has been shown to be a major determinant of different specificities between pepsin A and chymosin with site-directed mutagenesis (*36*), and other subsites, such as S3 and S2, are also expected to have significant roles in determining the unique specificities of various types of pepsins (*31*−*35*, *37*−*39*).

In the present study, the proteolytic specificities of canine pepsin B were investigated, in comparison with those of human pepsin A. Along with proteins such as hemoglobin and gelatin, octapeptides were used as substrates, choosing Lys-Pro-Ala-Glu-Phe-Phe-Arg-Leu as a parent peptide and substituting with various amino acids at P3, P2, P1′, and multiple positions. It was clarified here for the first time that pepsin B has a specificity very different from that of pepsin A, exclusively hydrolyzing peptides with Gly at P2. Because the occurrence of Tyr^{13} and Phe^{219} in/around the S2 subsite of pepsin B is quite unique, they were substituted by Ala and Ser, respectively, and vice versa in pepsin A by site-directed mutagenesis. The pepsin-B mutants, especially, the Tyr^{13}Ala/Phe^{219}Ser double-residue mutant, demonstrated pepsin-A-mimicking activity, hydrolyzing hemoglobin and various types of peptides efficiently, whereas this proteolytic activity was significantly decreased in pepsin A mutants. The structures of enzyme−substrate complexes were further investigated by molecular modeling analyses, to allow roles of Tyr^{13} and Phe^{219} to be discussed in detail.

EXPERIMENTAL PROCEDURES

Materials. The pYES2 cloning vector was purchased from Invitrogen Corp. Carlsbad, CA; the QuickChange site-directed mutagenesis kit from Stratagene, La Jolla, CA; the Y-PER yeast protein extraction reagent from Pierce Biotech, Inc., Rockford, IL; and glutathione Sepharose 4B and SP-Sephadex from Amersham Biosciences. Peptides were synthesized by Sigma Genosys Japan, Ishikari, Japan. All other chemicals were of reagent or analytical grade.

Assay of Proteolytic Activity. Proteolytic activity was determined with solutions of about 2% hemoglobin (*40*) and gelatin (*41*) as substrates, at pH 2 and 37 °C. Amounts of released peptides were determined by a fluorometric assay with fluorescamine (*42*).

Table 1: Hydrolytic Activities of Canine Pepsin B, Human Pepsin A, and Their Mutants Against Protein Substrates[a]

	activity (nmol min^{-1} (mg protein)$^{-1}$)[b]	
pepsin/mutant	hemoglobin	gelatin
pepsin B		
wild-type	11 ± 1	78 ± 21
Tyr^{13}Ala	**24 ± 1**	*12 ± 4*
Phe^{219}Ser	**21 ± 3**	*36 ± 6*
Tyr^{13}Ala/Phe^{219}Ser	**107 ± 9**	*33 ± 3*
pepsin A		
wild-type	360 ± 17	<4
Glu^{13}Tyr	*230 ± 6*	<4
Ser^{219}Phe	*46 ± 13*	uc[c]
Glu^{13}Tyr/Ser^{219}Phe	*27 ± 2*	uc

[a] The substrate protein (100 μL of a 2% m/v solution; pH was adjusted to 2.0 with HCl) was incubated with 10−30 ng of enzyme at 37 °C for 1−5 h. Reactions were stopped by the addition of 200 μL of 5% trichloroacetic acid in the case of hemoglobin (*40*), and 5 μL of a 5 M sodium-acetate buffer at pH 5, and 200 μL of isopropanol in the case of gelatin (*41*). An aliquot of the supernatant after centrifugation was subjected to a fluorometric assay with fluorescamine (*42*) to determine amounts of the released peptides. [b] The values for mutants that were significantly larger and smaller ($p < 0.05$) than those of the wild-type enzyme are shown in bold and italics, respectively. [c] uc: uncleaved.

Assay of Peptide Hydrolyzing Activity. Hydrolysis of peptides was assessed by methods described previously (*36*). In brief, the reaction mixture contained 0.2 M sodium forrmate buffer at pH 4, 50 μM of peptide, and an appropriate amount of enzyme. The total volume was 20 μL. After incubation at 37 °C for 1−6 h, the reaction was stopped by the addition of 80 μL of 3% perchloric acid. Following the removal of any precipitated material by centrifugation, reaction mixtures were subjected to HPLC on a column (0.46 cm i.d. × 25 cm) of ODS-120T (Tosoh Corp., Tokyo, Japan) that had been equilibrated with 0.1% trifluoroacetic acid. The column was eluted with a linear gradient of acetonitrile from 0 to 60% (v/v) over the course of 24 min in the presence of 0.1% trifluoroacetic acid at a flow rate of 0.8 mL/min. Quantification of peptides was carried out using their peak areas. The relative absorption coefficient at 214 nm of each peptide was calculated from the equation of Stephenson and Kenny (*43*).

Determination of Kinetic Parameters. The reaction mixture for determining the kinetic parameters for the cleavage of peptides contained 200 mM sodium formate buffer at pH 4, 0.5−5 ng of enzyme, and 10−120 μM substrate peptide in a total reaction volume of 50 μL. Incubation was done at 37 °C for 30 min and was stopped by the addition of 50 μL of 3% perchloric acid. The reaction was carried out in triplicate for each substrate concentration. Plots of $1/v$ against 1/[S] (Lineweaver−Burk) permitted the fitting of a straight line by linear regression, resulting in the determination of *K*m and *V*max. The *k*cat value was obtained with the equation for $V\text{max}/[E]_0$.

Expression and Purification of Canine Pepsinogen B, Human Pepsinogen A, and Their Mutants. cDNAs for canine pepsinogen B and human pepsinogen A have been molecularly cloned (*6*, *36*). Among the isozymogens identified in canine pepsinogen B, a cDNA for the major one (AB250936) was used. Site-directed mutagenesis was carried out accord-

Table 2: Hydrolytic Activities of Canine Pepsin B and Its Mutants against Typical Peptide Substrates

substrate	sequence and cleavage site[b]	activity (nmol min^{-1} (μg protein)$^{-1}$)[a]			
		wild-type	Tyr^{13}Ala	Phe^{219}Ser	Y^{13}A/F^{219}S
parent peptide	KPAEF↓FRL	uc[c]	**0.07 ± 0.02**	**0.02 ± 0.01**	**0.43 ± 0.05**
P3 variants					
Ile^3 variant	KP**I**EF↓FRL	uc	**0.09 ± 0.03**	**0.06 ± 0.02**	**0.13 ± 0.02**
Gly^3 variant	KP**G**EF↓FRL	uc	uc	**0.04 ± 0.01**	**0.17 ± 0.02**
Thr^3 variant	KP**T**EF↓FRL	uc	**0.04 ± 0.01**	**0.05 ± 0.02**	**0.17 ± 0.03**
Glu^3 variant	KP**E**EF↓FRL	0.04 ± 0.02	0.06 ± 0.02	**0.13 ± 0.03**	**0.30 ± 0.06**
Lys^3 variant	KP**K**EF↓FRL	0.04 ± 0.02	0.06 ± 0.02	**0.11 ± 0.02**	**0.27 ± 0.04**
P2 variants					
Leu^4 variant	KPA**L**F↓FRL	uc	uc	uc	**0.37 ± 0.02**
Val^4 variant	KPA**V**F↓FRL	uc	uc	uc	**0.06 ± 0.01**
Ala^4 variant	KPA**A**F↓FRL	uc	uc	**0.02 ± 0.01**	**0.16 ± 0.02**
Gly^4 variant	KPA**G**F↓FRL	0.14 ± 0.03	uc	0.12 ± 0.02	*0.07 ± 0.01*
Thr^4 variant	KPA**T**F↓FRL	uc	uc	uc	**0.06 ± 0.01**
Lys^4 variant	KPA**K**F↓FRL	uc	**0.13 ± 0.07**	**0.09 ± 0.04**	**0.24 ± 0.08**
P′1 variants					
Leu^6 variant	KPAEF↓**L**RL	0.03 ± 0.01	**0.16 ± 0.02**	**0.07 ± 0.02**	**1.3 ± 0.2**
Ile^6 variant	KPAEF↓**I**RL	uc	**0.05 ± 0.02**	uc	**0.33 ± 0.07**
Val^6 variant	KPAEF↓**V**RL	uc	uc	uc	**0.11 ± 0.02**
Ala^6 variant	KPAEF↓**A**RL	0.09 ± 0.02	**0.31 ± 0.06**	**0.26 ± 0.04**	**3.8 ± 0.5**
Gly^6 variant	KPAEF↓**G**RL	uc	uc	uc	**0.35 ± 0.05**
Thr^6 variant	KPAEF↓**T**RL	uc	uc	uc	**0.06 ± 0.02**
double-residue variants					
Gly^{3}Leu^6 variant	KP**G**EF↓**L**RL	uc	**0.06 ± 0.02**	**0.05 ± 0.01**	**0.51 ± 0.10**
Gly^{3}Ala^6 variant	KP**G**EF↓**A**RL	0.03 ± 0.01	**0.15 ± 0.03**	**0.09 ± 0.02**	**1.1 ± 0.3**
Leu^{4}Leu^6 variant	KPA**L**F↓**L**RL	uc	uc	uc	**0.52 ± 0.12**
Leu^{4}Ala^6 variant	KPA**L**F↓**A**RL	uc	**0.15 ± 0.05**	**0.06 ± 0.02**	**1.5 ± 0.3**
Ala^{4}Leu^6 variant	KPA**A**F↓**L**RL	uc	**0.03 ± 0.01**	**0.03 ± 0.01**	**0.22 ± 0.03**
Ala^{4}Ala^6 variant	KPA**A**F↓**A**RL	uc	**0.06 ± 0.02**	**0.03 ± 0.01**	**0.55 ± 0.08**
Gly^{4}Leu^6 variant	KPA**G**F↓**L**RL	3.1 ± 0.1	*0.05 ± 0.02*	*1.8 ± 0.2*	*0.24 ± 0.03*
Gly^{4}Val^6 variant	KPA**G**F↓**V**RL	0.29 ± 0.03	uc	*0.15 ± 0.03*	uc
Gly^{4}Ala^6 variant	KPA**G**F↓**A**RL	3.2 ± 0.3	*0.10 ± 0.03*	*2.6 ± 0.3*	*0.66 ± 0.07*
Gly^{4}Gly^6 variant	KPA**G**F↓**G**RL	0.38 ± 0.09	uc	*0.20 ± 0.05*	*0.07 ± 0.02*
Gly^{4}Thr^6 variant	KPA**G**F↓**T**RL	uc	uc	uc	uc
Thr^{4}Leu^6 variant	KPA**T**F↓**L**RL	uc	uc	uc	uc
Lys^{4}Leu^6 variant	KPA**K**F↓**L**RL	0.05 ± 0.01	0.09 ± 0.04	0.06 ± 0.02	**0.42 ± 0.02**
triple-residue variants					
Ile^{3}Gly^{4}Leu^6 variant	KP**IG**F↓**L**RL	2.0 ± 0.1	*0.12 ± 0.01*	*0.82 ± 0.03*	*0.21 ± 0.02*
Gly^{3}Gly^{4}Leu^6 variant	KP**GG**F↓**L**RL	3.6 ± 0.3	*0.07 ± 0.02*	*2.2 ± 0.1*	*0.15 ± 0.03*
Gly^{3}Gly^{4}Ala^6 variant	KP**GG**F↓**A**RL	3.7 ± 0.3	*0.14 ± 0.02*	*2.3 ± 0.1*	*0.24 ± 0.05*
Thr^{3}Gly^{4}Leu^6 variant	KP**TG**F↓**L**RL	2.9 ± 0.2	*0.08 ± 0.01*	*1.3 ± 0.1*	*0.18 ± 0.01*
Glu^{3}Gly^{4}Leu^6 variant	KP**EG**F↓**L**RL	4.0 ± 0.2	*0.14 ± 0.01*	*1.7 ± 0.2*	*0.31 ± 0.03*
Lys^{3}Gly^{4}Leu^6 variant	KP**KG**F↓**L**RL	2.5 ± 0.1	*0.07 ± 0.01*	*1.1 ± 0.1*	*0.19 ± 0.02*

[a] The values for mutants that were significantly larger or smaller ($p < 0.05$) than those of the wild-type enzyme are shown in bold and italics, respectively. [b] In the peptide sequences, replaced residues are shown in bold. [c] uc indicates that the peptide was uncleaved or that the rate of its hydrolysis gave a value less than 0.02 nmol min^{-1} (μg protein.)$^{-1}$.

ing to the manual for the QuickChange site-directed mutagenesis kit, employing a yeast expression system established previously (*36*). *S. cerevisiae* cells harboring pYES2-GSTF-zymogen plasmids were grown at 25−30 °C in shaker flasks in a synthetic medium without uracil. At a cell density of $A_{600} = 0.1$, the cells were harvested and shifted to an induction medium, which contained 2% galactose. After incubation for 4 days, the cultures were centrifuged to collect cells that were then lysed at room temperature for 30 min with 5 volumes of Y-PER solution containing 5 mM 2-mercaptoethanol and proteinase inhibitors (chymostatin, phosphoramidon, E-64, leupeptin, and antipain of 0.015, 0.2, 2, 0.1, and 0.4 mM, respectively). The Y-PER extract was mixed with an equal volume of 0.02 M sodium phosphate buffer containing 0.5 M NaCl and was applied to a column (0.7 i.d. × 0.5 cm) of glutathione Sepharose 4B equilibrated with 0.01 M sodium phosphate buffer at pH 7.0, containing 0.25 M NaCl. The column was washed with the equilibration buffer and then with the 0.05 M Tris-HCl buffer at pH 8.0. The adsorbed GST fusion protein was eluted with 1 mL of 0.05 M Tris-HCl buffer at pH 8.0, containing 10 mM reduced glutathione, and the eluate was mixed with an equal volume of glycerol and stored at −20 °C. Active enzymes were prepared by the activation of GST-fusion pepsinogen, with a procedure similar to that used with various pepsinogens previously (*36*, *44*). Briefly, a solution of GST-fusion pepsinogen was mixed with a one-fourth volume of 0.15 N HCl and incubated at 37 °C and 14 °C in the cases of pepsins B and A, respectively. The incubation time was varied from 20 min to 24 h to obtain the maximal amount of the active enzyme (*6*, *44*). After activation, 3 volumes of SP-Sephadex suspension (SP-Sephadex in 4 volumes of 0.05 M sodium acetate buffer at pH 5.0) were added, and the soluble fraction containing pepsin was collected by centrifugation.

Molecular Modeling. Tertiary structural models of canine pepsin B, human pepsin A, and their complexes with peptide

Table 3: Hydrolytic Activities of Human Pepsin A and Its Mutants against Typical Peptide Substrates

substrate	sequence and cleavage site[b]	activity (nmol min^{-1} (μg protein)$^{-1}$)[a] wild-type	Glu^{13}Tyr	Ser^{219}Phe	E^{13}Y/S^{219}F
parent peptide	KPAEF↓FRL	15.1 ± 1.3	*3.0 ± 0.2*	*0.19 ± 0.02*	*0.05 ± 0.01*
P3 variants					
Ile^3 variant	KP**I**EF↓FRL	18.0 ± 3.7	*1.6 ± 0.1*	*0.23 ± 0.01*	*0.04 ± 0.01*
Gly^3 variant	KP**G**EF↓FRL	15.3 ± 0.9	*2.2 ± 0.1*	*0.25 ± 0.01*	*0.04 ± 0.01*
Thr^3 variant	KP**T**EF↓FRL	6.5 ± 0.1	*0.63 ± 0.09*	*0.12 ± 0.03*	*0.06 ± 0.02*
Glu^3 variant	KP**E**EF↓FRL	7.2 ± 0.1	*1.1 ± 0.1*	*0.23 ± 0.05*	*0.13 ± 0.03*
Lys^3 variant	KP**K**EF↓FRL	0.35 ± 0.09	*0.22 ± 0.06*	*0.20 ± 0.05*	*0.10 ± 0.03*
P2 variants					
Leu^4 variant	KPA**L**F↓FRL	22.6 ± 2.2	*6.0 ± 0.4*	*0.13 ± 0.01*	*0.07 ± 0.01*
Val^4 variant	KPA**V**F↓FRL	13.6 ± 0.3	*3.3 ± 0.1*	*0.06 ± 0.01*	uc[c]
Ala^4 variant	KPA**A**F↓FRL	11.0 ± 0.7	*2.0 ± 0.2*	*0.17 ± 0.01*	*0.04 ± 0.01*
Gly^4 variant	KPA**G**F↓FRL	3.2 ± 0.3	*0.66 ± 0.04*	uc	uc
Thr^4 variant	KPA**T**F↓FRL	6.3 ± 0.1	*2.0 ± 0.2*	*0.06 ± 0.01*	uc
Lys^4 variant	KPA**K**F↓FRL	2.5 ± 0.1	*1.2 ± 0.2*	*0.15 ± 0.05*	*0.08 ± 0.02*
P′1 variants					
Leu^6 variant	KPAEF↓**L**RL	6.6 ± 0.1	*1.8 ± 0.3*	*0.06 ± 0.01*	uc
Ile^6 variant	KPAEF↓**I**RL	9.6 ± 1.4	*2.9 ± 0.3*	*0.27 ± 0.02*	*0.06 ± 0.01*
Val^6 variant	KPAEF↓**V**RL	4.9 ± 1.0	*2.4 ± 0.3*	*0.11 ± 0.01*	uc
Ala^6 variant	KPAEF↓**A**RL	2.9 ± 0.1	*0.74 ± 0.06*	uc	uc
Gly^6 variant	KPAEF↓**G**RL	uc	uc	uc	uc
Thr^6 variant	KPAEF↓**T**RL	1.2 ± 0.2	*0.32 ± 0.01*	uc	uc
double-residue variants					
Gly^{3}Leu^6 variant	KP**G**EF↓**L**RL	3.2 ± 0.1	*2.0 ± 0.1*	*0.09 ± 0.03*	uc
Gly^{3}Ala^6 variant	KP**G**EF↓**A**RL	0.89 ± 0.14	*0.37 ± 0.01*	uc	uc
Leu^{4}Leu^6 variant	KPA**L**F↓**L**RL	13.2 ± 0.2	*9.4 ± 0.7*	*0.12 ± 0.02*	*0.09 ± 0.01*
Leu^{4}Ala^6 variant	KPA**L**F↓**A**RL	8.8 ± 1.4	*1.5 ± 0.3*	*0.04 ± 0.01*	uc
Ala^{4}Leu^6 variant	KPA**A**F↓**L**RL	13.5 ± 0.4	*3.6 ± 0.6*	*0.06 ± 0.01*	*0.05 ± 0.01*
Ala^{4}Ala^6 variant	KPA**A**F↓**A**RL	2.5 ± 0.4	*0.70 ± 0.01*	uc	uc
Gly^{4}Leu^6 variant	KPA**G**F↓**L**RL	0.96 ± 0.10	*0.35 ± 0.04*	uc	uc
Gly^{4}Val^6 variant	KPA**G**F↓**V**RL	3.0 ± 0.1	*0.66 ± 0.02*	uc	uc
Gly^{4}Ala^6 variant	KPA**G**F↓**A**RL	0.79 ± 0.08	*0.19 ± 0.22*	uc	uc
Gly^{4}Gly^6 variant	KPA**G**F↓**G**RL	uc	uc	uc	uc
Gly^{4}Thr^6 variant	KPA**G**F↓**T**RL	0.19 ± 0.01	*0.04 ± 0.01*	uc	uc
Thr^{4}Leu^6 variant	KPA**T**F↓**L**RL	12.2 ± 1.8	*4.5 ± 0.2*	*0.20 ± 0.02*	*0.06 ± 0.01*
Lys^{4}Leu^6 variant	KPA**K**F↓**L**RL	1.4 ± 0.1	*0.75 ± 0.05*	*0.06 ± 0.02*	*0.05 ± 0.01*
triple-residue variants					
Ile^{3}Gly^{4}Leu^6 variant	KP**I**GF↓**L**RL	0.82 ± 0.04	*0.06 ± 0.01*	uc	uc
Gly^{3}Gly^{4}Leu^6 variant	KP**G**GF↓**L**RL	0.17 ± 0.02	*0.10 ± 0.01*	uc	uc
Gly^{3}Gly^{4}Ala^6 variant	KP**G**GF↓**A**RL	0.18 ± 0.02	*0.08 ± 0.01*	uc	uc
Thr^{3}Gly^{4}Leu^6 variant	KP**T**GF↓**L**RL	0.21 ± 0.04	uc	uc	uc
Glu^{3}Gly^{4}Leu^6 variant	KP**E**GF↓**L**RL	0.06 ± 0.02	uc	uc	uc
Lys^{3}Gly^{4}Leu^6 variant	KP**K**GF↓**L**RL	uc	uc	uc	uc

[a] The values for mutants that were significantly larger or smaller ($p < 0.05$) than those of the wild-type enzyme are shown in bold and italics, respectively. [b] In the peptide sequences, the replaced residues are shown in bold. [c] uc indicates that the peptide was uncleaved or that the rate of its hydrolysis gave a value less than 0.02 nmol min^{-1} (μg protein.)$^{-1}$.

substrates were constructed with the program Modeller (*45*), using crystal structures of the complex between human pepsin A and a synthetic phosphonate inhibitor (*46*), porcine pepsin A (*24*−*26*, *47*), bovine chymosin (*48*), and human progastricsin (*49*) and its intermediate (*50*) as the initial models. Images were created using RASMOL version 2.5. Hydrogen bonds of constructed models were defined as those interactions between donors and acceptors with a distance less than 3.5 Å, an angle at the hydrogen atom greater than 110° and the angle at the acceptor atom greater than 80°.

Statistics. All statistical analyses were performed using Statistica (StatSoft, Inc., Tulsa, OK). Data are presented as the mean ± SD, and statistical significance was determined with the Student's *t* test.

RESULTS AND DISCUSSION

Substrate Specificities of Pepsin B. Pepsin B hydrolyzed gelatin efficiently but scarcely hydrolyzed hemoglobin, in contrast to pepsin A, which hydrolyzed hemoglobin efficiently but was much less active against gelatin (Table 1). Although hemoglobin is a typical protein substrate for various proteinases, gelatin is unique because it is a thermal denaturation product of collagen rich in Gly and Pro. This specificity of pepsin B suggests that the enzyme is adapted to digest unique food proteins such as collagen, whereas the specificity of pepsin A is consistent with the fact that this pepsin is involved in the digestion of a variety of food proteins in the stomach. Table 2 summarizes the data for hydrolytic activities of pepsin B and its mutants against various octapeptides. The parent peptide chosen in this study, that is, KPAEFFRL, has been shown to be an ideal substrate for porcine pepsin A (*29*). The substrate set contained 37 peptides that were replaced at P3, P2, and P1′ with several typical residues, with respect to tolerance for larger to smaller hydrophobic (Phe, Leu, Ile, Val, Ala, and Gly), polar (Thr), or negatively (Glu) or positively (Lys) charged side chains.

Table 4: Kinetic Constants for the Hydrolysis of Typical Peptides by Canine Pepsin B and Its Mutants[a]

substrate, sequence, and cleavage site[b]		wild-type	Tyr[13]Ala	Phe[219]Ser	Y[13]A/F[219]S
parent peptide					
KPAEF↓FRL	*K*m		0.35 ± 0.05	0.42 ± 0.05	0.71 ± 0.10
	*k*cat	uc[c]	2.5 ± 0.4	1.2 ± 0.3	18 ± 5
	*k*cat/*K*m		***7.1 ± 0.5***	***2.8 ± 0.4***	***25 ± 2***
Ala[4] variant					
KPA**A**F↓FRL	*K*m			0.50 ± 0.05	0.67 ± 0.08
	*k*cat	uc	uc	1.2 ± 0.2	11 ± 3
	*k*cat/*K*m			***2.4 ± 0.5***	***16 ± 2***
Leu[6] variant					
KPAEF↓**L**RL	*K*m	>5	>5	>5	4.0 ± 0.5
	*k*cat				113 ± 15
	*k*cat/*K*m				***28 ± 3***
Ala[6] variant					
KPAEF↓**A**RL	*K*m	0.95 ± 0.10	>5	>5	1.3 ± 0.2
	*k*cat	3.4 ± 0.5			91 ± 18
	*k*cat/*K*m	3.6 ± 0.4			***73 ± 6***
Gly[3]Ala[6] variant					
KP**G**EF↓**A**RL	*K*m	>5	>5	>5	>5
	*k*cat				
	*k*cat/*K*m				
Gly[4]Ala[6] variant					
KPA**G**F↓**A**RL	*K*m	4.0 ± 0.6	>5	2.5 ± 0.4	>5
	*k*cat	169 ± 20		130 ± 30	
	*k*cat/*K*m	42 ± 5		51 ± 7	
Gly[3]Gly[4]Ala[6] variant					
KP**GG**F↓**A**RL	*K*m	2.2 ± 0.4	>5	2.2 ± 0.6	>5
	*k*cat	134 ± 23		116 ± 28	
	*k*cat/*K*m	60 ± 2		53 ± 2	

[a] All reactions were carried out in 0.2 M sodium formate buffer at pH 4.0. The units of *K*m, *k*cat, and *k*cat/*K*m are mM, s^{-1}, and mM^{-1} s^{-1}, respectively. The *k*cat/*K*m values for mutants that were found to be significantly larger or smaller ($p < 0.05$) than those of the wild-type enzymes are shown in bold and italics, respectively. [b] In the peptide sequence, the replaced residues are shown in bold. [c] uc indicates that the peptide was uncleaved or that the rate of its hydrolysis gave a value less than 0.02 nmol min^{-1} (μg protein.)$^{-1}$.

Pepsin B scarcely hydrolyzed the parent peptide and its single-residue variants, except that peptides with Glu/Lys at P3, Gly at P2, and Leu/Ala at P1′ were hydrolyzed very slowly. When octapeptides with Gly at P2 and Leu/Ala at P1′ such as KP**AG**F↓**A**RL (the cleavage site is shown by an arrow, and P3, P2, and P1′ residues are shown by bold letters) were used, remarkable activity of pepsin B was observed. With the Gly-Phe-Ala/Leu combination at P2 through P1′, P3 specificity was found to be low, and various types of residues, including hydrophobic, polar, and charged examples, were accommodated, although Glu/Lys was slightly more effective than other residues. Replacement of Gly at P2 with other residues such as Ala made peptides uncleavable, with very rigid P2 specificity. Regarding P1′, Ala and Leu were most preferred, followed by Gly and Val. Phe proved to be an unfavorable residue. This showed that, although P1′ specificity was less rigid, relatively small hydrophobic residues were preferred. Thus, X-Gly-Phe-Ala/Leu was the best combination at P3 through P1′. This preference is consistent with efficient hydrolysis of gelatin rich in Gly. It is notable that most peptides having Gly at P2 were hydrolyzed more efficiently by pepsin B than by pepsin A (Table 3). Kinetic analyses showed that catalysis by pepsin B is characterized by large *K*m and *k*cat values that reflect low affinity for a substrate and high turnover of the reaction, respectively. The *K*m values at pH 4 for KP**AG**F↓**A**RL and KP**GG**F↓**A**RL were 4.0 and 2.2 mM, respectively, and *k*cat values were 169 and 134 s^{-1} (Table 4). Thus, efficient hydrolysis by pepsin B might be mainly due to the rapid dissociation of the enzyme−substrate complexes.

Human pepsin A showed high activity against the parent octapeptide, KP**AE**F↓**F**RL (Table 3). At P3, various residues were accommodated except that Lys was unfavorable. Various residues were also accommodated at P2 in the order of Leu > Glu > Val > Ala > Thr > Gly > Lys, in contrast with the rigid specificity of pepsin B. When Gly was placed at P2, the rate of hydrolysis decreased to about one-fifth of that of the parent peptide. The activity against P1′ variants was inversely proportional to the size of the hydrophobic side chain of the P1′ residue, decreasing in the order of Phe > Ile > Leu > Val > Ala. When Gly was at P1′, the peptide was hardly hydrolyzed. These P1′ specificities were essentially different from that of pepsin B in that pepsin A preferred larger hydrophobic residues. Thus, the best peptides in the present set were KP**AL**F↓**F**RL, KP**IE**F↓**F**RL, KP**GE**F↓**F**RL and KP**AE**F↓**F**RL, and those having unfavorable combinations were KP**AE**F**G**RL and KP**AG**F**G**RL. The *K*m and *k*cat values at pH 4 for KP**AE**F↓**F**RL were about 50 μM and 40 s^{-1}, respectively (Table 5), roughly similar to those obtained for porcine pepsin A (*27*). By replacing P3 and P2 of the substrate with Gly, the *K*m value was increased and the *k*cat value decreased, resulting in a lowering of the hydrolytic activity.

Structural Features of Pepsin B, Molecular Models, and Addressing Sites for Mutagenesis. The present results on the specificity of pepsin B showed that the S2 subsite has an essential role. Because residues constituting the active site

Table 5: Kinetic Constants for the Hydrolysis of Typical Peptides by Human Pepsin A and Its Mutants[a]

substrate, sequence, and cleavage site[b]		wild-type	Glu[13]Tyr	Ser[219]Phe	E[13]Y/S[219]F
parent peptide					
KPAEF↓FRL	*K*m	0.058 ± 0.003	0.065 ± 0.009	1.5 ± 0.2	>2.5
	*k*cat	38 ± 4	6.4 ± 0.6	6.1 ± 0.5	
	*k*cat/*K*m	650 ± 100	*98 ± 5*	*8.7 ± 0.5*	
Ala[4] variant					
KPA**A**F↓FRL	*K*m	0.052 ± 0.003	0.061 ± 0.004	0.32 ± 0.05	0.24 ± 0.03
	*k*cat	15 ± 1	2.6 ± 0.1	1.2 ± 0.1	0.24 ± 0.04
	*k*cat/*K*m	290 ± 20	*42 ± 3*	*3.8 ± 0.2*	*0.99 ± 0.08*
Ala[6] variant					
KPAEF↓**A**RL	*K*m	0.24 ± 0.02	0.13 ± 0.02		
	*k*cat	19 ± 2	2.4 ± 0.2	uc[c]	uc
	*k*cat/*K*m	82 ± 16	*18 ± 1*		
Gly[3]Ala[6] variant					
KP**G**EF↓**A**RL	*K*m	0.21 ± 0.03	0.13 ± 0.01		
	*k*cat	3.6 ± 0.4	1.0 ± 0.1	uc	uc
	*k*cat/*K*m	17 ± 1	*8.0 ± 0.1*		
Gly[4]Ala[6] variant					
KPA**G**F↓**A**RL	*K*m	0.26 ± 0.02	0.13 ± 0.01		
	*k*cat	5.2 ± 0.3	0.59 ± 0.04	uc	uc
	*k*cat/*K*m	20 ± 3	*4.6 ± 0.5*		
Gly[3]Gly[4]Ala[6] variant					
KP**GG**F↓**A**RL	*K*m	0.23 ± 0.05	0.12 ± 0.01		
	*k*cat	0.86 ± 0.13	0.57 ± 0.03	uc	uc
	*k*cat/*K*m	3.8 ± 0. 2	4.7 ± 0.6		

[a] All reactions were carried out in 0.2 M sodium formate buffer at pH 4.0. The units of *K*m, *k*cat, and *k*cat/*K*m are mM, s^{-1}, and $mM^{-1}s^{-1}$, respectively. The *k*cat/*K*m values for mutants that were found to be significantly larger or smaller ($p < 0.05$) than those of the wild-type enzymes are shown in bold and italics, respectively. [b] In the peptide sequence, the replaced residues are shown in bold. [c] uc indicates that the peptide was uncleaved or that the rate of its hydrolysis gave a value less than 0.02 nmol min^{-1} (μg protein.)$^{-1}$.

have been anticipated from the tertiary structures of porcine (*23*−*26*) and human (*46*) pepsins A, human progastricsin (*49*, *50*), and bovine chymosin (*48*), they were compared with pepsin B and other types of pepsins. The sequence similarities of canine pepsin B with human pepsin A, gastricsin, and bovine chymosin are 49, 66, and 48%, respectively. Because the tertiary structure of pepsin B has hitherto not been clarified, it was constructed here by molecular modeling (Figure 1). Although the constructed structure of pepsin B was found to have good similarity with the X-ray structures of human and porcine pepsins A, conformational variability was observed in the loop regions forming the entrance of the active site, including the 107−118 and 238−246 loops (Figure 1B). This observation was also relevant in relation to the structures of other aspartic proteinases (*24*). Spatial arrangements of the active-site residues of pepsin B were estimated (Figures 1 and 2). The possible residues constituting the S2 subsite of pepsin B are Tyr[13], Gly[76], Ser[77], Gly[217], Thr[218], Thr[222], Glu[287], Thr[289], and Ile[300] (porcine pepsin-A numbering). When pepsin B accommodates Gly in the S2 subsite, residues interacting with the P2 main chain of a substrate are thought to be important because the side chain of Gly is only a hydrogen atom. Between residues in the S2 subsite, the former 5 residues possibly interact with the P2 main chain (*46*, *51*). Although they are well conserved or replaced with equivalent residues, the occurrence of Tyr[13] in pepsin B is exceptional because less bulky residues, such as Glu, Ala, and Gln, are common in other pepsins. The phenol side chain of Tyr[13] extends to the S2 subsite and might contact with the P2 main chain of a substrate, as shown in the constructed model (Figure 2A). Tyr[13] locates at a position symmetrical to that of Tyr[189], which is an important residue in the S1′ and S2′ subsites, associated with the active-site aspartates (Figure 3A). Tyr[13] and Tyr[189] have been shown to be topologically equivalent on the basis of the gene duplication hypothesis (*52*). Another remarkable residue in the active site of pepsin B is Phe[219]. Its occurrence is very exceptional because Ser[219] is common in all other pepsins. Because Ser[219] has shown to be important to the formation of the active-site hydrogen bond network (*38*), its replacement with Phe might be expected to have a significant affect on catalytic activity. Thus, positions 13 and 219 were chosen as targeting sites. Mutations in pepsin B were performed to replace Tyr[13] and Phe[219] with Ala and Ser, respectively, and those in pepsin A were performed to replace Glu[13] and Ser[219] with Tyr and Phe, respectively. The choice of Ala at position 13 in pepsin B was thought to be appropriate because Ala[13] is frequent in other pepsins, and the size of its side chain is small.

Change in Substrate Specificity with Mutations. Significant changes in protein and peptide hydrolysis were observed between wild-type and mutant enzymes (Tables 1−3). The hemoglobin digestive activities of Tyr[13]Ala and Phe[219]Ser mutants and the Tyr[13]Ala/Phe[219]Ser double-residue mutants of pepsin B increased by factors of 2.2, 1.9, and 9.7, respectively. The reverse results were obtained in the case of gelatin. Hemoglobin digestive activities of Glu[13]Tyr and Ser[219]Phe mutants and the Glu[13]Ala/Ser[219]Phe double-residue mutant of pepsin A were decreased by factors of 1.6, 7.8, and 13, respectively. However, gelatinolytic activity did not appear in pepsin-A mutants. Although the hemoglobin digestive activity of pepsin B was hardly detectable, the activity of the Tyr[13]Ala/Phe[219]Ser-pepsin B was elevated to one-third of that of pepsin A, showing that the characteristic of pepsin B was changed to a pepsin-A-mimicking one by the double mutation.

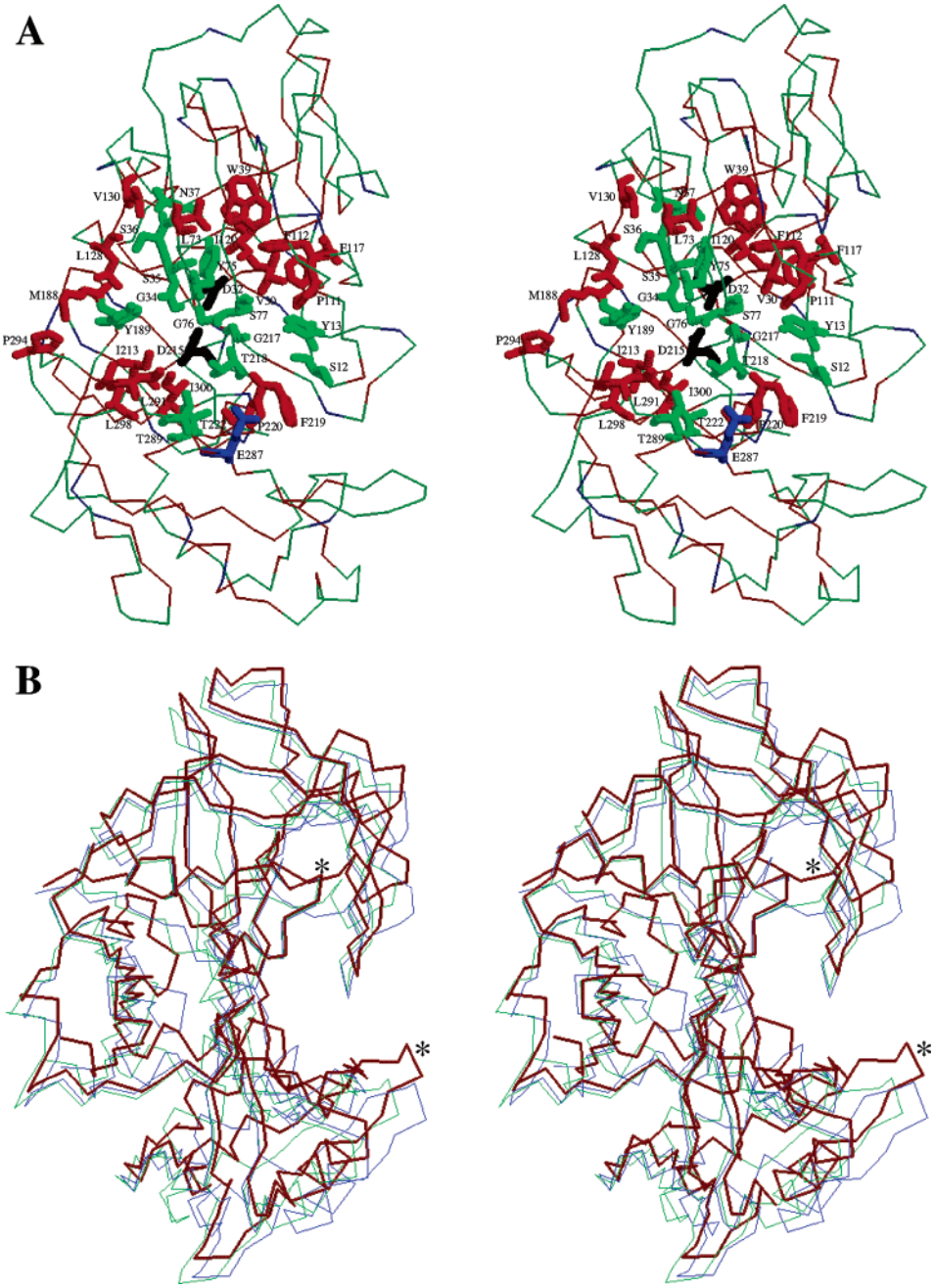

FIGURE 1: Stereoviews of the tertiary structures of canine pepsin B. (A) Highlighting the S4−S3′ subsites and catalytic site aspartates. Residues are shown with wireframes, distinguished by red, green, and blue colors for nonpolar hydrophobic, polar but uncharged, and charged residues, respectively. Catalytic site aspartates are shown in black. Putative residues in the S4 through S3′ subsites are shown with thick wireframes. Except for the expected residues in the S4−S3′ subsites, only backbone atoms are given. Porcine pepsin-A numbering is used. (B) The left-side view of A. The structure of canine pepsin B is shown with backbone atoms only (red), superimposed on the structures of human (blue) and porcine (green) pepsin A forms. Asterisks show typical conformational variability in the 107−118 (upper) and 238−246 (lower) loops among the three pepsins.

The Tyr[13]Ala mutant of pepsin B demonstrated new hydrolytic activity against several peptides, whereas the activity against peptides with Gly at P2 was decreased significantly (Table 2). However, because the newly obtained activity of the Tyr[13]Ala mutant was, in fact, found to be low, the mutant is a rather poor enzyme. Nonetheless, from this mutant, it is clear that the occurrence of Tyr[13] is essential for the accommodation of Gly at P2. The Phe[219]Ser mutant exhibited similar broad activity against various peptides, with retention of high activity against peptides with Gly at P2. This showed that the occurrence of Phe[219] is not essential for the accommodation of Gly at P2 but is a hindrance to the hydrolysis of various peptides of other types. The significant modification of specificity was achieved by the Tyr[13]Ala/Phe[219]Ser double-residue mutation. The mutant demonstrated general proteolytic activity, hydrolyzing various types of peptides very efficiently, although activity against peptides with Gly at P2 was decreased. The activity against typical peptides, such as KP**A**EF↓**A**RL, KP**A**EF↓**L**RL, and KP**GE**F↓**A**RL, was increased about 40 times by the double mutation, the extent being much higher than that with single mutations. In contrast, in the case of pepsin A, the cleavage rate was significantly decreased for all peptides by a factor of 1.6−11 in the Glu[13]-Tyr mutant, by more than 28 in the Ser[219]Phe mutant, and

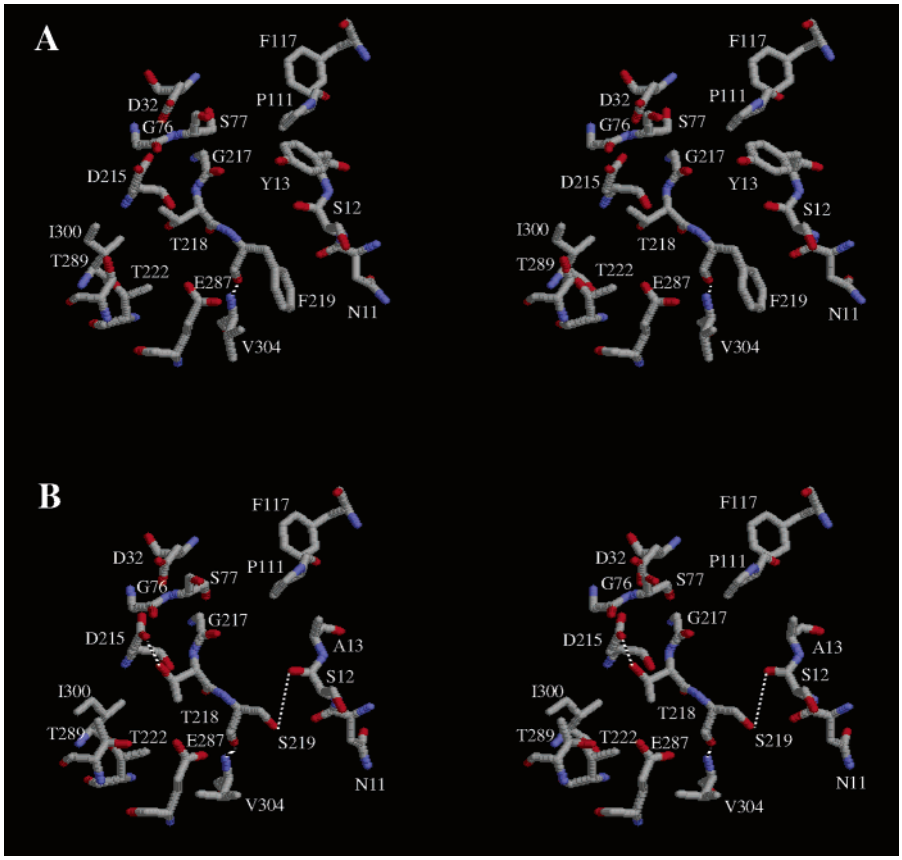

FIGURE 2: Stereoviews of the tertiary structures of the S3 and S2 subsites of canine pepsin B (A) and its Tyr[13]Ala/Phe[219]Ser double-residue mutant (B). Selected residues including catalytic site aspartates and residues in the S3 and S2 subsites are given. The residues are shown with thick wireframes, distinguished by gray, red, and light-blue colors for carbon, oxygen, and nitrogen, respectively. The possible hydrogen-bonding intramolecular interactions between Asp[215] and Thr[218], Ser[219] and Ser[12], and Ser/Phe[219] and Val[304] are shown by dotted white lines. Although the distance between Ser[219] OH and Ser[12] O is 3.7 Å, the hydroxyl turns around the dihedral angle $\chi 1$ to form a hydrogen bond with Ser[12] O in substrate-binding models, and therefore, this value is given as a potential hydrogen-bonding distance. Porcine pepsin-A numbering is used.

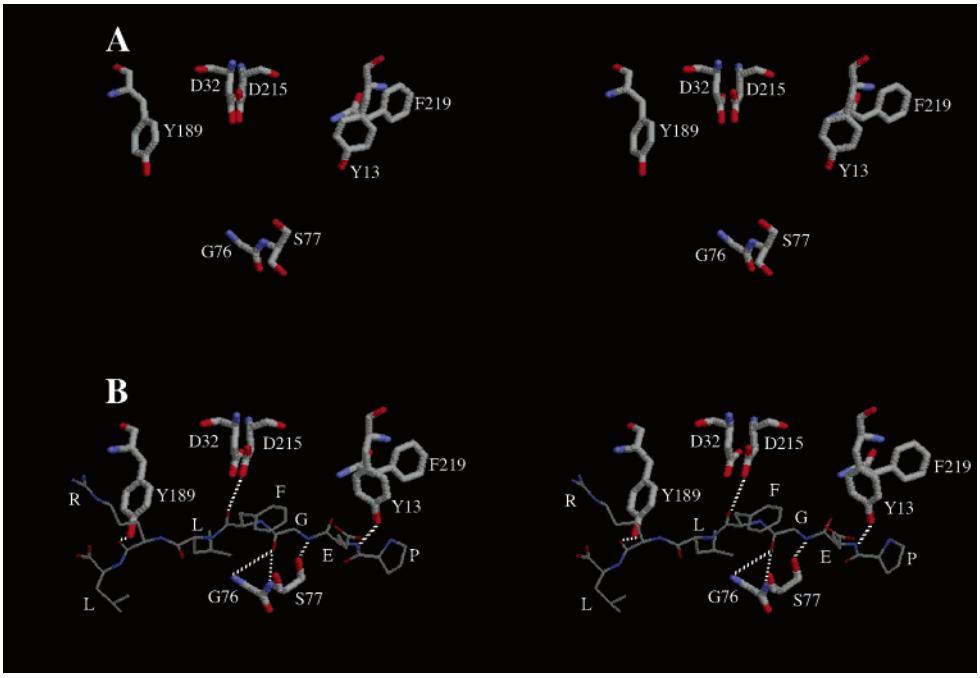

FIGURE 3: Stereoviews of active-site aspartates and subsite residues of pepsin B without (A) and with (B) the substrate, PEGFLRL. Only residues possibly contacting with the main chain of the substrate are shown. Possible hydrogen bonds are shown with dotted white lines. Porcine pepsin-A numbering is used.

by more than 100 in the double mutant (Table 3). Although Tyr[13] in pepsin B was shown to be essential for the exclusive accommodation of Gly in the S2 subsite, Glu[13]Tyr pepsin A did not exhibit such unique specificity.

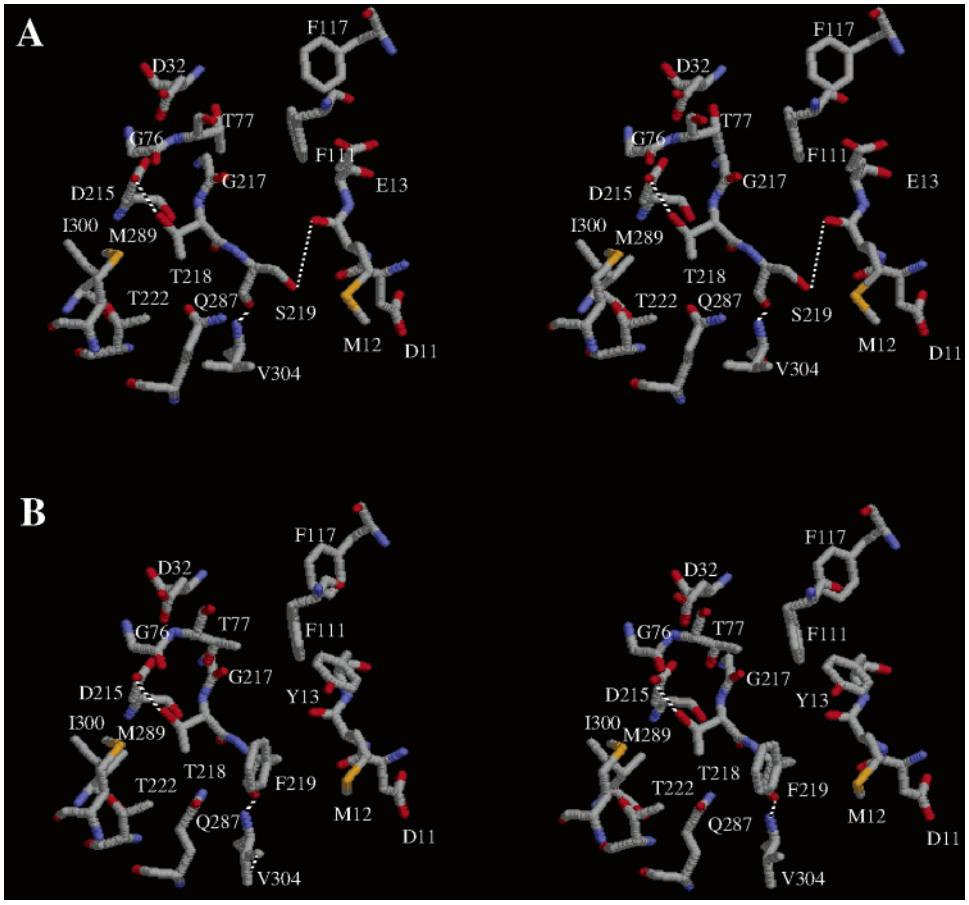

FIGURE 4: Stereoviews of the tertiary structures of the S3 and S2 subsites of human pepsin A (A) and its Glu[13]Tyr/Ser[219]Phe double-residue mutant (B). Residues are shown with thick wireframes, distinguished by gray, red, light-blue, and orange colors for carbon, oxygen, nitrogen, and sulfur atoms, respectively. The possible hydrogen-bonding intramolecular interactions between Asp[215] and Thr[218], Ser[219] and Met[12], and Ser/Phe[219] and Val[304] are shown by dotted white lines. Although the distance between Ser[219] OH and Met[12] O is 3.9 Å, the hydroxyl turns around the dihedral angle $\chi 1$ to form a hydrogen bond with Met[12] O in substrate-binding models as found in a crystal structure of the complex between human pepsin A and a synthetic inhibitor (*46*), and therefore, this value is given as a potential hydrogen-bonding distance.

Michaelis−Menten kinetics with typical peptides was examined. Pepsin B and its mutants showed occasionally high *K*m values. Although the Tyr[13]Ala/Phe[219]Ser double mutant of pepsin B demonstrated high hydrolytic activity against various types of peptides, except those with Gly at P2, it was clear that the *k*cat value was increased significantly in each case, resulting in an increase in the specificity constant (*k*cat/*K*m) (Table 4). In pepsin A, the *K*m values for peptides with Gly at P3 and P2 did not change or were decreased by the Glu[13]Tyr mutation. The Ser[219]Phe mutation affected both *K*m and *k*cat values, resulting in a marked decrease in hydrolytic activity. These effects of mutations were amplified in the Glu[13]Tyr/Ser[219]Phe double mutant of pepsin A, which had very low hydrolytic activity (Table 5).

Roles of Tyr[13] and Phe[219] in the Substrate Specificity of Pepsin B. Here, Tyr[13] and Phe[219] were found to be responsible for the specific preference of pepsin B for peptides with Gly at P2. Especially, Tyr[13] is of prime importance. Molecular modeling of pepsin B indicates that the phenol moiety of Tyr[13] occupies the substrate-binding space around the S2/S3 subsite (Figures 1 and 2). Access of the substrate might be hindered with such a geometry, which might force the exclusive accommodation of Gly at P2 because Gly is very flexible and allows substrates to be accommodated in a narrow active site. The flexibility of Gly has been shown to be essential when Gly-rich substrates are hydrolyzed by metalloproteinases such as elastase (*53*). In a molecular model binding a substrate, PEGFLRL, the phenol moiety of Tyr[13], moves from its initial position (Figure 3B). In this location, Tyr[13] OH forms a hydrogen bond with P3 N of the substrates. Because the hydroxyl of Tyr[189], which is highly conserved among pepsins, forms a hydrogen bond with P2′ O, it is notable that these two symmetrical Tyr OHs tightly fix the main chain of a substrate at the most distant positions from the catalytic site (Figure 3B). These hydrogen bonds and those between Gly[76] N and P2 O, Ser[77] N and P2 O, and Ser[77] OH and P2 N are the major hydrogen bonds fixing the peptide main chain to the active site. Hydrogen bonds interacting with the main chain of a substrate have been analyzed by site-directed mutagenesis of aspartic proteinases. Position 77 is commonly occupied by Thr, and its mutagenic conversion to a hydrophobic amino acid has been shown to lower the catalytic activity (*34*, *35*, *38*, *47*, *54*). Furthermore, with complexes of pepsin B and a substrate, plots of phi/psi angles of the substrate showed only those of a residue at P2 to be located near the boundary of the favorable region (data not shown), suggesting that the flexibility of the main chain conformation is low at P2. This also indicates that Gly is more acceptable at P2 than other residues because of its flexibility. When Tyr[13] is replaced with Ala, the spatial limitation and the rigidity at P2 is weakened, and various residues can be accommodated.

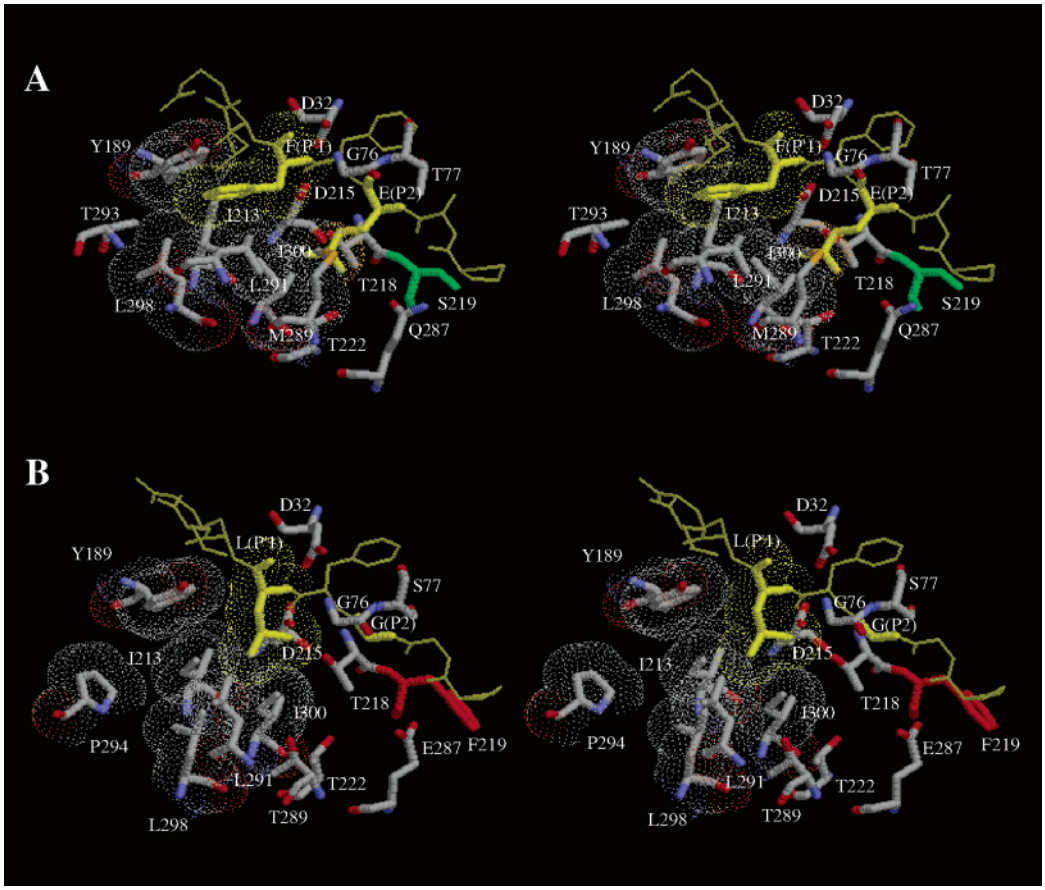

FIGURE 5: Stereoviews of the spatial arrangement of the residues in S2 and S1′ subsites of human pepsin A (A) and canine pepsin B (B) in complex with their respective preferred hexapeptide substrates, i.e., PAEFFRL (A) and PGGFLRL (B). Residues are shown with thick wireframes, distinguished by gray, red, light-blue, and orange colors for carbon, oxygen, nitrogen, and sulfur, respectively. Atoms of substrates are colored yellow and with thin wireframes except for those of P2 and P1′ residues, which are with thick wireframes. Ser and Phe at residue 219 are shown in green and red, respectively. Because van der Waals surface forces are known to have significant roles in the attraction of hydrophobic residues, they are given here as dots for hydrophobic residues and Tyr^{189} in the putative S2 and S1′ subsites, and the P2 and P1′ residues of substrates. Porcine pepsin-A numbering is used.

The occurrence of Phe^{219} in pepsin B is also unique because position 219 is occupied by Ser in all other pepsins. Hydrogen bonds formed by Ser^{219} O^{γ} with Thr^{12} O, and Ser^{219} O with Val^{304} N have been shown to contribute to the conformational stability of the active site in porcine pepsin A (*38*), making the Thr^{218}−Ser^{219} main chain parallel with the substrate main chain, supporting S3 and S2 subsite contacts with P3 and P2 substrate residues, respectively, as well as assisting the formation of a hydrogen-bonding interaction between Thr^{218} $O^{\gamma 1}$ and Asp^{215} $O^{\delta 2}$, which is important for catalytic activity at low pH (*47*). Replacement of Ser^{219} with Ala in porcine pepsin A lowered the activity, probably because of the loss of hydrogen bonding (*38*). In wild-type pepsin B, the hydrogen-bonding network in the active site is weak because Phe^{219} cannot form a hydrogen bond, provisionally causing the low hydrolytic activity of pepsin B against various peptides. The replacement of Phe^{219} with Ser by mutation would be expected to regenerate a hydrogen bond. However, the change in proteolytic specificity was incomplete with the Phe^{219}Ser single-residue mutant, the Tyr^{13} being thought to have significant influence on enzyme activity. Marked change in proteolytic specificity and the resulting increase in general proteolytic activity was thus achieved by the Tyr^{13}Ala/Phe^{219}Ser double mutation. The structural change in the active site of pepsin B due to the Tyr^{13}Ala/Phe^{219}Ser mutation is shown Figure 2B. The replacement of Tyr^{13} by Ala results in the appearance of a wide area accommodating a substrate. A new hydrogen bond from Ser^{219} O^{γ} to Ser^{12} O might be formed, contributing to the conformational stability of the active site including S3 and S2. These changes in the active site are expected to result in an increase in general proteolytic activity.

Reverse mutation in pepsin A made the enzyme less active/inactive, but the Glu^{13}Tyr mutation did not endow specificity for Gly at P2 (Table 3). The conformation of Tyr^{13} is different from the case of pepsin B, occupying a significant part of the S3 subsite (Figure 4). This conformation might depend on the sheet structure of the *N*-terminal residues of pepsin A. Under this geometry of Tyr^{13}, the phenol OH cannot form a hydrogen bond with P3 N/O of the substrate main chain, whereas the steric hindrance of the phenol moiety might be effective in lowering the catalytic activity against all types of peptides. The Ser^{219}Phe mutation lowered the activity much more effectively than the Glu^{13}Tyr mutation. In this mutant, the phenyl side chain of Phe^{219} is present as an unusual rotamer, occupying the substrate binding space so that access to the active site might be hindered, although the collapse of the hydrogen bond from Ser^{219} O^{γ} to Met^{12} O might also be important (Figure 4). Substrates might be blocked from access to the active site. These show that the spatial arrangement of the bulky side chains of Tyr^{13} and Phe^{219} in mutant pepsin A is not constructed in the same

way as that in pepsin B. Because these conformations of the side chains of Tyr^{13} and Phe^{219} are similar in the Glu^{13}-$Tyr/Ser^{219}Phe$ double-residue mutant, this would also explain the significant decrease in the hydrolytic activity of the double-residue mutant.

Although activity of the $Tyr^{13}Ala/Phe^{219}Ser$ mutant of pepsin B against peptides with Phe at P1′ was lower than that of pepsin A, with peptides with Ala or Gly at P1′ it was comparable to or larger than activity of pepsin A. This might reflect differences in the P1′ subsite between pepsins B and A. Pepsin B prefers small hydrophobic residues, such as Ala and Leu at P1′, whereas pepsin A (*9*, *22*) prefers bulky hydrophobic residues such as Phe. Molecular models of binding with substrate peptides show the differences in P1′ specificity rather clearly (Figure 5). S1′ residues consist of conserved residues, including Tyr^{189}, Ile^{213}, and Ile^{300}, and group-specific residues located in the 289−299 loop (*36*). Pepsin B has a spatial distribution of group-specific residues different from those of pepsin A. As a result, the hydrophobic residues in the S1′ subsite, except Pro^{294} located at the boundary of the S1′ subsite, distribute compactly in pepsin B but are expanded in pepsin A. Thus, the S1′ subsite of pepsin B preferentially accommodates small hydrophobic residues, consistent with the present experimental results. Bulky hydrophobic residues, such as Phe and Trp, are accommodated predominantly in the S1′ subsite of pepsin A as reported by Fruton (*9*) and clarified in the present study. Differences in the spatial distribution of S1′ residues might be due to variation in the length of the S1′ loop. A short loop makes the S1′ subsite more open and wide, as found in chymosin (*48*). The long loop resulting from the one-residue insertion in pepsin B contributes to the formation of the compact S1′ subsite.

Conclusions. The unique hydrolytic specificity of pepsin B, accommodating Gly at P2 nearly exclusively, and preferring small hydrophobic residues at P1′, was clarified here for the first time by systematic analyses with octapeptide substrates. Because pepsin A is known to be a typical model of proteolytic enzymes because of extensive studies on its structure and catalytic properties (*10*−*12*), comparative elucidation of the structural origin of the unique specificity of pepsin B is clearly advantageous, contributing to the elucidation of the structural and functional relationships of aspartic proteinases. Tyr^{13} and Phe^{219} of pepsin B were found to be involved in the specificity for accommodating Gly exclusively at P2. The rigid specificity was canceled, and general proteolytic activity was conferred by replacing them with Ala and Ser, respectively.

SUPPORTING INFORMATION AVAILABLE

PDB files of canine pepsin B in complex with/without the heptapeptide, PEGFLRL. This material is available free of charge via the Internet at http://pubs.acs.org.

REFERENCES

1. Tang, J., Sepulveda, P., Marciniszyn, J., Jr., Chen, K. C., Huang, W. Y., Tao, N., Liu, D., and Lanier, J. P. (1973) Amino-acid sequence of porcine pepsin, *Proc. Natl. Acad. Sci. U.S.A. 70*, 3437−3439.
2. Foltmann, B. (1970) Prochymosin and chymosin, *Methods Enzymol. 19*, 421−436.
3. Foltmann, B. (1981) Gastric proteinases - structure, function, evolution and mechanism of action, *Essays Biochem. 17*, 52−84.
4. Kageyama, T., and Takahashi, K. (1986) The complete amino acid sequence of monkey progastricsin, *J. Biol. Chem. 261*, 4406−4419.
5. Kageyama, T., Tanabe, K., and Koiwai, O. (1990) Structure and development of rabbit pepsinogens. Stage-specific zymogens, nucleotide sequences of cDNAs, molecular evolution, and gene expression during development, *J. Biol. Chem. 265*, 17031−17038.
6. Narita, Y., Oda, S., Moriyama, A., and Kageyama, T. (2002) Primary structure, unique enzymatic properties, and molecular evolution of pepsinogen B and pepsin B, *Arch. Biochem. Biophys. 404*, 177−185.
7. Kageyama, T. (2002) Pepsinogens, progastricsins, and prochymosins: structure, function, evolution, and development, *Cell. Mol. Life Sci. 59*, 288−306.
8. Herriott, R. M. (1962) Pepsinogen and pepsin, *J. Gen. Physiol. 45*, 57−76.
9. Fruton, J. S. (1970) The specificity and mechanism of pepsin action, *Adv. Enzymol. Relat. Areas Mol. Biol. 33*, 401−443.
10. Davies, D. R. (1990) The structure and function of the aspartic proteinases, *Annu. Rev. Biophys. Biophys. Chem. 19*, 189−215.
11. Dunn, B. M. (2002) Structure and mechanism of the pepsin-like family of aspartic peptidases, *Chem. Rev. 102*, 4431−4458.
12. Fruton, J. S. (2002) A history of pepsin and related enzymes, *Q. Rev. Biol. 77*, 127−147.
13. Foltmann, B. (1992) Chymosin: a short review on foetal and neonatal gastric proteases, *Scand. J. Clin. Lab. Invest. 52* (Suppl 210), 65−79.
14. Tang, J. (1970) Gastricsin and pepsin, *Methods Enzymol. 19*, 406−421.
15. Ryle, A. P., and Porter, R. R. (1959) Parapepsins: two proteolytic enzymes associated with porcine pepsin, *Biochem. J. 73*, 75−86.
16. Ryle, A. P. (1965) Pepsinogen B: the zymogen of pepsin B, *Biochem. J. 96*, 6−16.
17. Ryle, A. P. (1970) The porcine pepsins and pepsinogens, *Methods Enzymol. 19*, 316−336.
18. Nielsen, P. K., and Foltmann, B. (1995) Purification and characterization of porcine pepsinogen B and pepsin B, *Arch. Biochem. Biophys. 322*, 417−422.
19. Suchodolski, J. S., Steiner, J. M., Ruaux, C. G., Boari, A., and Williams, D. A. (2002) Purification and partial characterization of canine pepsinogen A and B, *Am. J. Vet. Res. 63*, 1585−1590.
20. Shaw, B., and Wright, C. L. (1976) The pepsinogens of cat gastric mucosa and the pepsins derived from them, *Digestion. 14*, 142−152.
21. Sampath-Kumar, P. S., and Fruton, J. S. (1974) Studies on the extended active sites of acid proteinases, *Proc. Natl. Acad. Sci. U.S.A. 71*, 1070−1072.
22. Powers, J. C., Harley, A. D., and Myers, D. V. (1977) Subsite specificity of porcine pepsin, *Adv. Exp. Med. Biol. 95*, 141−157.
23. Andreeva, N. S., Zdanov, A. S., Gustchina, A. E., and Fedorov, A. A. (1984) Structure of ethanol-inhibited porcine pepsin at 2-Å resolution and binding of the methyl ester of phenylalanyl-diiodotyrosine to the enzyme, *J. Biol. Chem. 259*, 11353−11365.
24. Sielecki, A. R., Fedorov, A. A., Boodhoo, A., Andreeva, N. S., and James, M. N. (1990) Molecular and crystal structures of monoclinic porcine pepsin refined at 1.8 Å resolution, *J. Mol. Biol. 214*, 143−170.
25. Abad-Zapatero, C., Rydel, T. J., and Erickson, J. (1990) Revised 2.3 Å structure of porcine pepsin: evidence for a flexible subdomain, *Proteins 8*, 62−81.
26. Cooper, J. B., Khan, G., Taylor, G., Tickle, I. J., and Blundell, T. L. (1990) X-ray analyses of aspartic proteinases. II. Three-dimensional structure of the hexagonal crystal form of porcine pepsin at 2.3 Å resolution, *J. Mol. Biol. 214*, 199−222.
27. Dunn, B. M., Jimenez, M., Parten, B. F., Valler, M. J., Rolph, C. E., and Kay, J. (1986) A systematic series of synthetic chromophoric substrates for aspartic proteinases, *Biochem. J. 237*, 899−906.
28. Dunn, B. M., Valler, M. J., Rolph, C. E., Foundling, S. I., Jimenez, M., and Kay, J. (1987) The pH dependence of the hydrolysis of chromogenic substrates of the type, Lys-Pro-Xaa-Yaa-Phe-(NO_2)-Phe-Arg-Leu, by selected aspartic proteinases: evidence for specific interactions in subsites S3 and S2, *Biochim. Biophys. Acta 913*, 122−130.
29. Dunn, B. M., and Hung, S. (2000) The two sides of enzyme-substrate specificity: lessons from the aspartic proteinases, *Biochim. Biophys. Acta 1477*, 231−240.

30. Lin, X. L., Wong, R. N., and Tang, J. (1989) Synthesis, purification, and active site mutagenesis of recombinant porcine pepsinogen, *J. Biol. Chem. 264*, 4482−4489.
31. Suzuki, J., Sasaki, K., Sasao, Y., Hamu, A., Kawasaki, H., Nishiyama, M., Horinouchi, S., and Beppu, T. (1989) Alteration of catalytic properties of chymosin by site-directed mutagenesis, *Protein Eng. 2*, 563−569.
32. Shintani, T., Nomura, K., and Ichishima, E. (1997) Engineering of porcine pepsin. Alteration of S1 substrate specificity of pepsin to those of fungal aspartic proteinases by site-directed mutagenesis, *J. Biol. Chem. 272*, 18855−18861.
33. Williams, M. G., Wilsher, J., Nugent, P., Mills, A., Dhanaraj, V., Fabry, M., Sedlacek, J., Uusitalo, J. M., Penttila, M. E., Pitts, J. E., and Blundell, T. L. (1997) Mutagenesis, biochemical characterization and X-ray structural analysis of point mutants of bovine chymosin, *Protein Eng. 10*, 991−997.
34. Okoniewska, M., Tanaka, T., and Yada, R. Y. (1999) The role of the flap residue, threonine 77, in the activation and catalytic activity of pepsin A, *Protein Eng. 12*, 55−61.
35. Okoniewska, M., Tanaka, T., and Yada, R. Y. (2000) The pepsin residue glycine-76 contributes to active-site loop flexibility and participates in catalysis, *Biochem. J. 349*, 169−177.
36. Kageyama, T. (2004) Role of S′1 loop residues in the substrate specificities of pepsin A and chymosin, *Biochemistry 43*, 15122−15130.
37. Strop, P., Sedlacek, J., Stys, J., Kaderabkova, Z., Blaha, I., Pavlickova, L., Pohl, J., Fabry, M., Kostka, V., Newman, M., Frazao, C., Shearer, A., Tickle, I. J., and Blundell, T. L. (1990) Engineering enzyme subsite specificity: preparation, kinetic characterization, and X-ray analysis at 2.0- Å resolution of Val111Phe site-mutated calf chymosin, *Biochemistry 29*, 9863−9871.
38. Lin, Y., Fusek, M., Lin, X., Hartsuck, J. A., Kezdy, F. J., and Tang, J. (1992) pH dependence of kinetic parameters of pepsin, rhizopuspepsin, and their active-site hydrogen bond mutants, *J. Biol. Chem. 267*, 18413−18418.
39. Pitts, J. E., Dhanaraj, V., Dealwis, C. G., Mantafounis, D., Nugent, P., Orprayoon, P., Cooper, J. B., Newman, M., and Blundell, T. L. (1992) Multidisciplinary cycles for protein engineering: site-directed mutagenesis and X-ray structural studies of aspartic proteinases, *Scand. J. Clin. Lab. Invest. 52* (Suppl 210), 39−50.
40. Anson, M. L., and Mirsky, A. E. (1932) The estimation of pepsin with hemoglobin, *J. Gen. Physiol. 16*, 59−63.
41. Jones, B. L., Fontanini, D., Jarvinen, M., and Pekkarinen, A. (1998) Simplified endoproteinase assays using gelatin or azogelatin, *Anal. Biochem. 263*, 214−220.
42. De Bernardo, S., Weigele, M., Toome, V., Manhart, K., Leimgruber, W., Böhlen, P., Stein, S., and Udenfriend, S. (1974) Studies on the reaction of fluorescamine with primary amines, *Arch. Biochem. Biophys. 163*, 390−399.
43. Stephenson, S. L., and Kenny, A. J. (1987) Metabolism of neuropeptides. Hydrolysis of the angiotensins, bradykinin, substance P and oxytocin by pig kidney microvillar membranes, *Biochem. J. 241*, 237−247.
44. Kageyama, T., and Takahashi, K. (1980) Monkey pepsinogens and pepsins. IV. The amino acid sequence of the activation peptide segment of Japanese monkey pepsinogen, *J. Biochem. 88*, 9−16.
45. Sali, A., and Blundell, T. L. (1993) Comparative protein modelling by satisfaction of spatial restraints, *J. Mol. Biol. 234*, 779−815.
46. Fujinaga, M., Cherney, M. M., Tarasova, N. I., Bartlett, P. A., Hanson, J. E., and James, M. N. (2000) Structural study of the complex between human pepsin and a phosphorus-containing peptidic-transition-state analog, *Acta Crystallogr., Sect. D 56*, 272−279.
47. Andreeva, N. S., and Rumsh, L. D. (2001) Analysis of crystal structures of aspartic proteinases: on the role of amino acid residues adjacent to the catalytic site of pepsin-like enzymes, *Protein Sci. 10*, 2439−2450.
48. Newman, M., Safro, M., Frazao, C., Khan, G., Zdanov, A., Tickle, I. J., Blundell, T. L., and Andreeva, N. (1991) X-ray analyses of aspartic proteinases. IV. Structure and refinement at 2.2 Å resolution of bovine chymosin, *J. Mol. Biol. 221*, 1295−1309.
49. Moore, S. A., Sielecki, A. R., Chernaia, M. M., Tarasova, N. I., and James, M. N. (1995) Crystal and molecular structures of human progastricsin at 1.62 Å resolution, *J. Mol. Biol. 247*, 466−485.
50. Khan, A. R., Khazanovich-Bernstein, N., Bergmann, E. M., and James, M. N. (1999) Structural aspects of activation pathways of aspartic protease zymogens and viral 3C protease precursors, *Proc. Natl. Acad. Sci. U.S.A. 96*, 10968−10975.
51. Fujinaga, M., Chernaia, M. M., Tarasova, N. I., Mosimann, S. C., and James, M. N. (1995) Crystal structure of human pepsin and its complex with pepstatin, *Protein Sci. 4*, 960−972.
52. Tang, J., James, M. N., Hsu, I. N., Jenkins, J. A., and Blundell, T. L. (1978) Structural evidence for gene duplication in the evolution of the acid proteases, *Nature 271*, 618−621.
53. Vessillier, S., Delolme, F., Bernillon, J., Saulnier, J., and Wallach, J. (2001) Hydrolysis of glycine-containing elastin pentapeptides by LasA, a metalloelastase from Pseudomonas aeruginosa, *Eur. J. Biochem. 268*, 1049−1057.
54. Galea, C. A., Dalrymple, B. P., Kuypers, R., and Blakeley, R. (2000) Modification of the substrate specificity of porcine pepsin for the enzymatic production of bovine hide gelatin, *Protein Sci. 9*, 1947−1959.

BI061467A